Analytical Methods

Accepted Manuscript

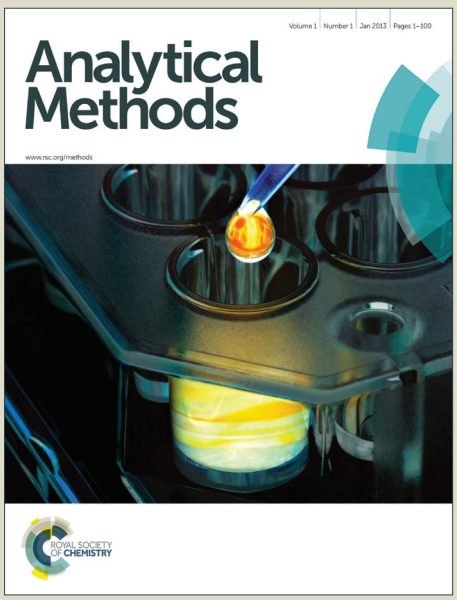

ROYAL SOCIETY OF CHEMISTRY

www.rsc.org/methods

Analytical Methods

RSCPublishing

ARTICLE

Graphene/Au composites as an anode modifier for improving electricity generation in *Shewanella*-inoculated microbial fuel cells

Cui-e Zhao,[a] Panpan Gai,[a] Rongbin Song,[a] Jianrong Zhang*[a, b] and Jun-Jie Zhu*[a]

Cite this: DOI: 10.1039/xoxxoooooox

Received ooth January 2015,
Accepted ooth January 2015

DOI: 10.1039/xoxxoooooox

www.rsc.org/

The electricity generation in microbial fuel cells (MFCs) greatly depends on anode materials, which directly affect bacterial attachment on the anode surface and extracellular electron transfer (ETT) between microorganisms and electrode. Herein, the graphene/Au (G/Au) composites were used as a novel anode material in *Shewanella*-inoculated MFC. The current generation and power density of the MFC with the G/Au modified carbon paper (CP/G/Au) anode were significantly improved compared with conventional carbon paper (CP) anode. This could be attributed to the large surface area, excellent conductivity and good biocompatibility for enhanced bacterial loading on the anode surface and improved EET efficiency between microbe and electrode.

Introduction

Microbial fuel cells (MFCs) have emerged as a promising technology for the electricity generation and wastewater treatment *via* microbial metabolism. [1-4] However, the practical applications of MFCs still face a lot of challenges due to the relatively low power output resulting from the low bacterial loadings and extracellular electron transfer (EET) efficiency. Usually, the performance of MFCs is affected by several factors such as pH, temperature, external resistance, microbial type and anode material. [5-7] In particular, the anode materials directly affect the attachment of bacterial cells, electron transfer and substrate oxidation, remaining one of the most important factors that limit the power density of MFCs. [8-10] Commonly used materials include carbon-based electrodes, such as carbon paper, carbon cloth and graphite felt due to their good chemical stability. However, these materials usually exhibit poor bacterial adhesion and low EET efficiency. One promising approach to improve anode performance is to modify carbon electrodes with conductive polymers or nanomaterials. [11-16]

Recently, graphene has attracted tremendous attention in a great variety of areas, such as energy storage, electro-catalysts, and biosensor because of its excellent mechanical and electrical properties. [17-19] Furthermore, graphene can serve as an ideal two-dimension nanostructure of substrates for the fabrication of composite materials due to its large surface area. [20-23] As well known, gold nanoparticles (AuNPs) have many unique properties such as good biocompatibility, conductivity and stability, showing a great potential of application for MFCs. [24-27] For instance, Sun et al. have reported that the introduction of gold layer on carbon paper significantly enhance the MFC performance. Thus, the coupling of graphene and AuNPs provides an effective strategy to further increase the electricity generation. However, there is rarely works regarding the application of graphene/Au for MFCs anode material.

In this study, the graphene/Au (G/Au) composites were used as a novel anode material for *shewanella*-inoculated MFCs. The current generation and power density of the G/Au-modified carbon paper (CP/G/Au) anode were greatly enhanced compared with conventional carbon paper (CP) anode. The improved performance could be attributed to the increased active surface area, excellent conductivity and good biocompatibility for the attachment of bacterial cells on the CP/G/Au anode surface and improved EET efficiency between bacteria and electrode.

Experimental

Preparation and characterization of the G/Au composites

Graphene (G) was prepared through the reduction of graphene oxide (GO) *via* the modified Hummer method,[28, 29] while the G/Au composites were synthesized according to a previous report. [30] Briefly, 30 uL of ammonium hydroxide and

a State Key Laboratory of Analytical Chemistry for Life Science, School of Chemistry and Chemical Engineering, Nanjing University; Nanjing 210093, P. R. China.
E-mail: jrzhang@nju.edu.cn; jjzhu@nju.edu.cn;
b School of Chemistry and Life Science, Nanjing University Jinling college, Nanjing 210089, P. R China

10 mg of sodium borohydride were added into 10 mL of 1 mg mL^{-1} GO suspension, following by heating at 95 °C for 1 h. Then, 5 mL of 1% (wt.%) $HAuCl_4$ and 1 mL of 0.1 M sodium citrate were added dropwise into 5 mL of 0.7 mg mL^{-1} graphene colloid solution, respectively. Then the solution was stirred at 60 °C for 2 h. The morphology and nanostructures of the samples were characterized by scanning electron microscope (SEM) and X-ray diffraction (XRD). The G or G/Au modified carbon paper (CP/G, CP/G/Au) electrode was fabricated by dripping G or G/Au solution on both sides of CP (6 cm^2) with a loading of ~ 0.5 mg/cm^2.

MFCs construction and measurements

H-shaped MFC was constructed by connecting two glass bottles of 100 mL. The CP, CP/G, and CP/G/Au electrodes with the same area (6 cm^2) were installed in the same anode chamber without contact between each other, whereas the CP was used as the cathode. The *Shewanella oneidensis* cells were inoculated into the MFC anode chamber with 18 mM lactate as the sole electron donor. The cells cultivation and anolyte preparation were the same as those of a previous report. [31] The anode and the cathode were connected to the external circuit using titanium wire with a fixed external resistance of 1000 Ω. The MFCs were operated at 25 °C under N_2 atmosphere.

The polarization and power density curves were obtained by varying the external resistance (R) (50–10,000Ω) applied to the circuit. Current (I) was calculated as $I = E/R$, and power (P) were calculated as $P = I \times E$, where E is the cell voltage. The current and power densities were then normalized to anode surface area. Electrochemical impedance spectroscopy (EIS) was carried out with an Autolab PGSTAT12 (Eco chemie, BV, The Netherlands) at open-circuit potential. The frequency range was between 10^{-2} and 10^5 Hz. Cyclic voltammetry (CV) was performed using a CHI660D workstation (Chenhua, China) with a saturated calomel electrode (SCE) reference electrode and a Platinum counter electrode. For SEM (HITACHI S4800) observation, small pieces of anodes were scarified and fixed in 2.5% glutaraldehyde for 2h, dehydrated in series of ethanol solution (25%, 50%, 75%, 95%, and 100%), and then vacuum dried. Samples were coated with Au prior to the SEM observation.

Results and discussion

Characterization of the G/Au composites

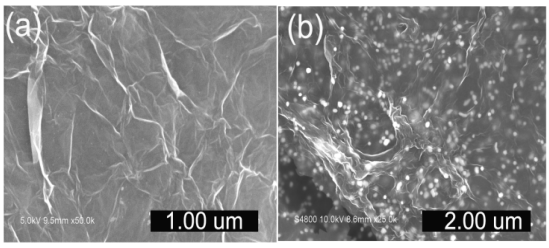

Fig. 1 SEM images of (a) the G and (b) the G/Au composites.

Fig. 1a showed a typical SEM image of graphene, exhibiting a flexible structure with some corrugated nanosheets. The image of the G/Au was presented in Fig. 1b, from which we could clearly see that a large number of AuNPs were uniformly distributed on the surface of the G sheets.

The XRD analysis was performed to study the crystal structure of the samples, as shown in Fig. 2. It could be seen that the diffraction peak of GO appeared at 2θ = 10.0° and then shifted to a higher angle after reduction at 2θ = 23.5°, which was assigned as (002) diffraction of the G. The crystallinity of AuNPs was evidenced by clear peaks at 2θ = 38.2°, 44.5°, 64.5° and 77.5°, corresponding to the (111), (200), (220) and (311) planes of the AuNPs. [30] The results further confirmed that AuNPs were successfully formed on the G surface.

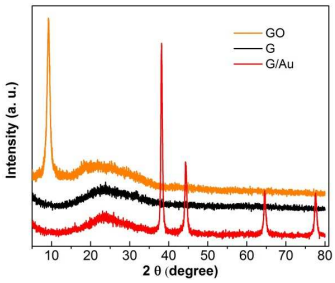

Fig. 2 XRD patterns of the GO, the G and the G/Au composites.

Characterization of the CP/G/Au electrode

After coated with G or G/Au composites, it was noted that the surface of the CP electrode was well decorated with the G or the G/Au (Fig. 3a and 3b) through π–π electronic interactions. [32, 33]

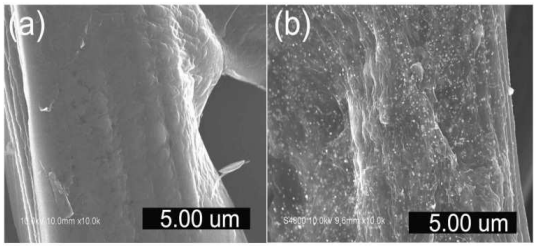

Fig. 3 SEM images of (a) the CP/G and (b) the CP/G/Au electrodes.

The electrochemical properties of the CP, the CP/G and the CP/G/Au electrodes were studied by CV, as shown in Fig. 4a. It was noted that the quasi-reversible one-electron redox behaviour of ferricyanide ions was observed on the CP/G or the CP/G/Au electrode, whereas no obvious redox peaks were observed on the CV plot of the CP electrode. Moreover, the peak current of $Fe(CN)_6^{3-/4-}$ relative to the CP/G or CP/G/Au electrode was much higher than that of the CP. Based on the Cottrell equation, with the same projected surface area, the active surface area of the CP/G or CP/G/Au electrode was relatively larger, which was expected to be beneficial to

bacterial attachment and electron collection from mediators excreted by *shewanella*. [34] In addition, the peak current of the CP/G/Au electrode was relatively higher than that of the CP/G electrode due to the large surface and high conductivity of AuNPs, indicating that the introduction of AuNPs played an important role in improving electron transfer.

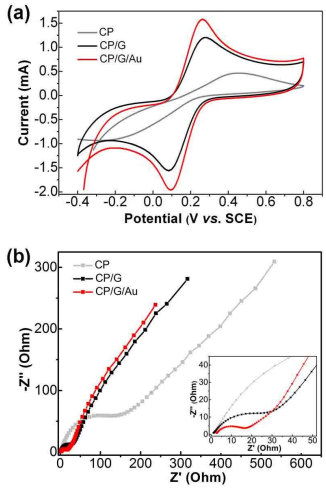

Fig. 4 (a) CV plots of the CP, the CP/G and the CP/G/Au electrodes in 5.0 mM $Fe(CN)_6^{3-/4-}$ and 0.1 M Na_2SO_4 solution at a scan rate of 10 mV s^{-1}; (b) Nyquist plots of different electrodes at open-circuit potential, the inset is the higher-magnification.

EIS was also an efficient tool to study the interface properties of surface-modified electrodes. [35] Thus, the capability of electron transfer of three electrodes was further investigated by EIS test (Fig. 4b). The charge-transfer resistance (R_{ct}) at an electrode/electrolyte interface was usually indicated by the diameter of the semicycle in the Nyquist curve. It was found that the CP/G and the CP/G/Au electrode had an R_{ct} of 31 Ω and 18 Ω, respectively, which was much lower than that of the CP electrode (~185 Ω). A smaller charge-transfer resistance was resulted from a faster electron transfer. [31] Therefore, the EET efficiency of the CP/G/Au electrode was greatly enhanced, indicating that it would be a promising candidate for MFCs anode.

The performance of the CP/G/Au anode in MFCs

To evaluate the performance of anodic materials, the biocurrent generation in three MFCs was recorded versus time, as shown in Fig. 5a. It was obvious that the current production was greatly affected by the modifying materials of the anodes. The CP/G/Au anode had a current density of over 750 mA m^{-2}, which was about 0.6 and 4.0 times higher than the CP/G (~ 450 mA m^{-2}) and CP (~ 150 mA m^{-2}) anode respectively, suggesting that the CP/G/Au anode produced more energy from the same mass of substrate.

To further understand the influence of anodic material on the MFC performance, the polarization curves and power density curves were evaluated. As shown in Fig. 5b, the maximum power density of the CP/G/Au anode was 508 mW m^{-2}, which was 1.8 and 3.1 times of those obtained with the CP/G (276 mW m^{-2}) and CP (162 mW m^{-2}) anodes, respectively. The high current density and power output from the CP/G/Au anode could be attributed to the large specific surface area and excellent conductivity for the enhanced bacterial loading and EET efficiency, as well as good biocompatibility for bacterial adhesion.

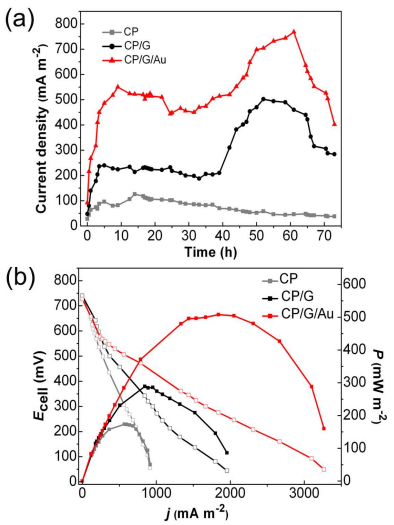

Fig. 5 (a) Current generation curves of MFCs with an external resistance of 1000 Ω, (b) Polarization and power density curves for three MFCs.

To test the merits of CP/G/Au electrode for microbial electricity generation, it was used as an anode at 0.2 V (vs. Ag/AgCl) in a three-electrode electrochemical cell (EC) system. [20] For comparison, the CP, the CP/Au, the CP/G electrodes were used as anodes, respectively. The current generation from ECs was shown in Fig. 6a. It was noted that the CP/G/Au anode generated a current density as high as 1800 mA m^{-2}, which was much higher than that of the CP electrode (200 mA m^{-2}). However, for the CP/Au and the CP/G electrode, the current density was 350 mA m^{-2} and 650 mA m^{-2}, respectively. The large surface area and high conductivity of CP/G/Au anode may play important roles in accepting electrons from riboflavin molecules and facilitating EET.

However, the increase in current production was also likely resulted from direct electron transfer between bacterial biofilm and CP/G/Au anode. To confirm this, four anodes were analysed using CV, respectively. As shown in Figure 6b, no obvious redox peaks were observed in the CV plot of the CP anode. For the CP/Au and the CP/G, a weak pair of redox peaks were observed at about -0.46 and -0.37 V (vs. Ag/AgCl), which were believed to originate from the c-type cytochromes of *Shewanella* for direct electron transfer. The CV of the CP/G/Au anode exhibited one well-defined pair of redox peaks at about -0.45 and -0.38 V, which were in accordance with the electrochemical response of outer-membrane proteins of *Shewanella*.[36-38] Furthermore, the peak current of the CP/G/Au anode was much higher than that of the other three anodes, indicated a synergistic effect between Au and G for increased EET efficiency.

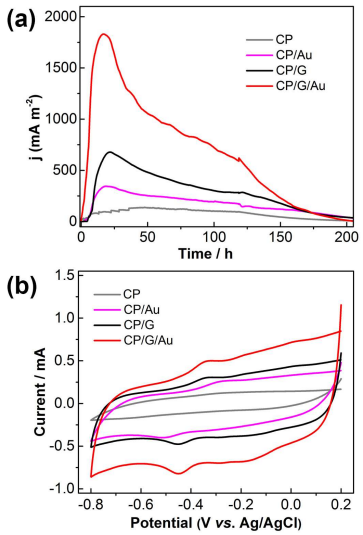

Fig. 6 Current generation (a), CV plots (b) with the CP, the CP/Au, the CP/G and the CP/G/Au anodes in EC systems.

To confirm the above findings, the bacterial loading of anodes in MFCs was observed by SEM. It could be seen that only a few bacterial cells were scattered on CP anode surface (Fig. 7a). In comparison, more bacterial cells were attached on CP/G anode surface (Fig. 7b). It was interesting to note that bacterial cells were accumulated on CP/G/Au anode surface and adhered to each other to form bacterial biofilm (Fig. 7c). The results indicated that the G/Au composites could improve bacterial loadings, which was due to the synergistic effects between G and AuNPs. On one hand, the G sheets served as a substrate to load AuNPs, which had large surface area for bacterial adhesion and electron collections from mediators in solution. On the other hand, the AuNPs exhibited favorable properties of high conductivity and good biocompatibility, which facilitated the EET, resulting in increased electricity generation and power output.

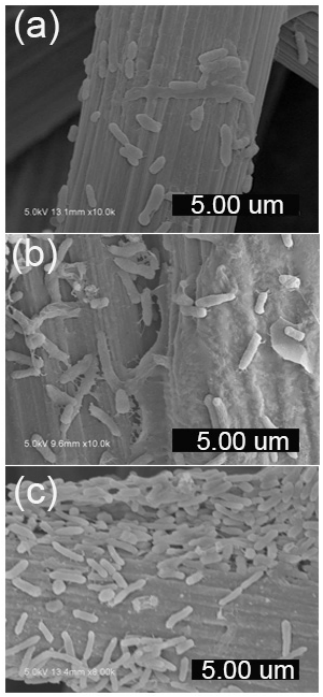

Fig. 7 SEM images of bacterial cells attached on the surface of (a) the CP, (b) the CP/G and (c) the CP/G/Au anodes.

Conclusions

In summary, the G/Au composites were successfully used as an anode material for MFCs. The performance of the MFC with the CP/G/Au anode was significantly improved compared with the CP, the CP/Au and the CP/G anodes, which was attributed to synergistic effects of G sheets and AuNPs resulted from the increased active surface area, excellent conductivity and good biocompatibility for the attachment of bacterial cells and electron transfer between bacteria and the electrode.

Acknowledgements

We gratefully appreciate the National Natural Science Foundation (21175065, 21375059, 21121091, 21335004). We also thank the support of the National Basic Research Program of China (2011CB933502).

Notes and references

1. D. R. Lovley, *Nat Rev Microbiol*, 2006, **4**, 497-508.
2. B. E. Logan, B. Hamelers, R. Rozendal, U. Schröder, J. Keller, S. Freguia, P. Aelterman, W. Verstraete and K. Rabaey, *Environ. Sci. Technol.*, 2006, **40**, 5181-5192.
3. Y. Qiao, S. J. Bao and C. M. Li, *Energy Environ. Sci.*, 2010, **3**, 544-553.
4. B. E. Logan, *Nat Rev Microbiol*, 2009, **7**, 375-381.
5. P. Aelterman, M. Versichele, M. Marzorati, N. Boon and W. Verstraete, *Bioresour. Technol.*, 2008, **99**, 8895-8902.
6. P. Aelterman, K. Rabaey, H. T. Pham, N. Boon and W. Verstraete, *Environ. Sci. Technol.*, 2006, **40**, 3388-3394.
7. H. Liu, S. Cheng and B. E. Logan, *Environ. Sci. Technol.*, 2005, **39**, 5488-5493.
8. Y. Liu, F. Harnisch, K. Fricke, U. Schröder, V. Climent and J. M. Feliu, *Biosens. Bioelectron.*, 2010, **25**, 2167-2171.
9. Z. He, J. Liu, Y. Qiao, C. M. Li and T. T. Y. Tan, *Nano Lett.*, 2012, **12**, 4738-4741.
10. S. Chen, G. He, A. A. Carmona-Martinez, S. Agarwal, A. Greiner, H. Hou and U. Schröder, *Electrochem. Commun.*, 2011, **13**, 1026-1029.
11. T. Zhang, Y. Zeng, S. Chen, X. Ai and H. Yang, *Electrochem. Commun.*, 2007, **9**, 349-353.
12. Y. Zhang, G. Mo, X. Li, W. Zhang, J. Zhang, J. Ye, X. Huang and C. Yu, *J. Power Sources*, 2011, **196**, 5402-5407.
13. B. Lai, X. Tang, H. Li, Z. Du, X. Liu and Q. Zhang, *Biosens. Bioelectron.*, 2011, **28**, 373-377.
14. J. Hou, Z. Liu and P. Zhang, *J. Power Sources*, 2013, **224**, 139-144.
15. Z. Wen, S. Ci, S. Mao, S. Cui, G. Lu, K. Yu, S. Luo, Z. He and J. Chen, *J. Power Sources*, 2013, **234**, 100-106.
16. L. Peng, S.-J. You and J.-Y. Wang, *Biosens. Bioelectron.*, 2010, **25**, 1248-1251.

17. C. Xu, B. Xu, Y. Gu, Z. Xiong, J. Sun and G. Zhao, *Energy & Environmental Science,* 2013, **6**, 1388-1414.
18. J.-F. Wu, M.-Q. Xu and G.-C. Zhao, *Electrochem. Commun.*, 2010, **12**, 175-177.
19. H. Yuan and Z. He, *Nanoscale*, 2015, DOI: 10.1039/C4NR05637J.
20. C. Zhao, P. Gai, C. Liu, X. Wang, H. Xu, J.-R. Zhang and J.-J. Zhu, *J. Mater. Chem. A*, 2013, **1**, 12587-12594.
21. X. Xin, X. Zhou, J. Wu, X. Yao and Z. Liu, *ACS Nano*, 2012, **6**, 11035-11043.
22. Y. Wu, Z. Wen, H. Feng and J. Li, *Chem. – A Eur. J.*, 2013, **19**, 5631-5635.
23. S. Wang and R. A. W. Dryfe, *J. Mater. Chem. A*, 2013, **1**, 5279-5283.
24. V. B. Wang, N. Yantara, T. M. Koh, S. Kjelleberg, Q. Zhang, G. C. Bazan, S. C. J. Loo and N. Mathews, *Chem. Commun.*, 2014, **50**, 8223-8226..
25. J. Han, Y. Zhuo, Y.-Q. Chai, L. Mao, Y.-L. Yuan and R. Yuan, *Talanta*, 2011, **85**, 130-135.
26. X. Wang, J. Dong, H. Ming and S. Ai, *Analyst*, 2013, **138**, 1219-1225.
27. M. Yang, B. G. Choi, T. J. Park, N. S. Heo, W. H. Hong and S. Y. Lee, *Nanoscale*, 2011, **3**, 2950-2956.
28. Y. Xu, H. Bai, G. Lu, C. Li and G. Shi, *J. Am. Chem. Soc.*, 2008, **130**, 5856-5857.
29. D. Li, M. B. Muller, S. Gilje, R. B. Kaner and G. G. Wallace, *Nat Nano*, 2008, **3**, 101-105.
30. Y. Chen, Y. Li, D. Sun, D. Tian, J. Zhang and J.-J. Zhu, *J. Mater. Chem.*, 2011, **21**, 7604-7611.
31. C. Zhao, Y. Wang, F. Shi, J. Zhang and J.-J. Zhu, *Chem. Commun.*, 2013, **49**, 6668-6670.
32. X. Xie, G. Yu, N. Liu, Z. Bao, C. S. Criddle and Y. Cui, *Energy Environ. Sci.*, 2012, **5**, 6862-6866.
33. P. Wu, Q. Shao, Y. Hu, J. Jin, Y. Yin, H. Zhang and C. Cai, *Electrochim. Acta*, 2010, **55**, 8606-8614.
34. E. Marsili, D. B. Baron, I. D. Shikhare, D. Coursolle, J. A. Gralnick and D. R. Bond, *Proc. Natl. Acad. Sci. U. S. A.*, 2008, **105**, 3968-3973.
35. Z. He and F. Mansfeld, *Energy Environ. Sci.*, 2009, **2**, 215-219.
36. Y. Qiao, X.-S. Wu and C. M. Li, *J. Power Sources*, 2014, **266**, 226-231.
37. X. Liu, W. Wu and Z. Gu, *J. Power Sources*, 2015, **277**, 110-115.
38. C. e. Zhao, J. Wu, Y. Ding, V. B. Wang, Y. Zhang, S. Kjelleberg, J. S. C. Loo, B. Cao and Q. Zhang, *ChemElectroChem*, 2015, DOI: 10.1002/celc.201402458.